Enhancement of the Absorption Coefficient of *cis*-$(NCS)_2$ Bis(2,2′-bipyridyl-4,4′-dicarboxylate)ruthenium(II) Dye in Dye-Sensitized Solar Cells by a Silver Island Film

Manabu Ihara,*,† Kanako Tanaka,† Keiji Sakaki,† Itaru Honma,‡ and Koichi Yamada†

Department of Chemical System Engineering, Faculty of Engineering, University of Tokyo, 7-3-1 Hongo, Bunkyo-ku, Tokyo 113, Japan, and Energy Division, Electrotechnical Laboratory, AIST, Umezono 1-1-4, Tsukuba, Ibaraki 305, Japan

Received: November 26, 1996[⊗]

The absorption coefficient of the dye used in dye-sensitized solar cells is a major factor in the total energy efficiency of the cell. In this work, we increased the absorption coefficient of the dye *cis*-$(NCS)_2$ bis(2,2′-bipyridyl-4,4′-dicarboxylate)ruthenium(II) used in such cells by having the dye adsorbed on silver islands. We studied the effect of the surface area of silver (per surface area of substrate) and the effect of dye concentration on this enhancement. This technique significantly enhanced the absorption coefficient of the Ru-dye for the metal−ligand charge-transfer transition, which generates electrons and holes in dye-sensitized solar cells. The enhancement ratio of the absorption was controlled by the amount of Ru-dye directly adsorbed on the silver islands. The absorption was enhanced by a factor of 149, which was achieved for a dye concentration of 3×10^{-10} mol/cm^2 and an average surface area of silver island of 0.63 cm^2/cm^2 of substrate. Such enhancement is expected to be useful in improving the electric energy conversion efficiency of dye-sensitized solar cells.

Introduction

Global warming is caused by the increase in CO_2 emissions. Because the electric power generation sector is one of the largest CO_2 sources, we need to develop a electricity generation system that emits less CO_2 than current systems. Solar cells are the preferred technology because they emit no CO_2 except during the fabrication process. Conventional solar cells generate electricity using semiconductor junctions, where the electrical energy conversion efficiency is very sensitive to the crystallinity and to the amount of defects and impurities. Accordingly, the fabrication of such cells requires expensive apparatus, such as a high-vacuum system, thus making the cost of electricity generated by these cells expensive.

Grätzel et al. developed a nanocrystalline dye-sensitized solar cell, called the Grätzel cell, that can be fabricated by the wet method, which is simple and inexpensive.[1−5] Sunlight is absorbed by the dye and generates electrons and holes, and the separated electrons are then injected into the TiO_2 nanocrystalline film while the holes are transported to the I^-/I_3^- solution. The maximum electric energy conversion efficiency is reported to be 10% when the dye used is *cis*-$(NCS)_2$ bis(2,2′-bipyridyl-4,4′-dicarboxylate)ruthenium(II).

In Grätzel solar cells, the incident monochromatic photon-to-current conversion efficiency (IPCE) determines the electric energy conversion efficiency, and in turn the IPCE is determined by the photon absorption of the dye, the injection of electrons into TiO_2 film, and the recombination of electrons and holes. A key factor in improving the electric energy conversion efficiency of this solar cell is a high absorption coefficient of the dye.

Dyes adsorbed on fine metallic islands, such as silver or gold, significantly enhance Raman scattering, because of the strong surface plasmon excitation.[6−15] This surface enhanced-Raman scattering (SERS) effect is closely related to the enhancement of optical properties, such as the absorption coefficient[16−22] Unfortunately, there are few experimental results on the absorption enhancement of dyes.[19]

In this work, we significantly increased the absorption coefficient of the dye *cis*-$(NCS)_2$ bis(2,2′-bipyridyl-4,4′-dicarboxylate) ruthenium(II), hereafter called Ru-dye, used in Grätzel cells by having it adsorbed on fine silver (Ag) islands. We studied the effect of both of the surface area of silver islands and the Ru-dye concentration on the enhancement. From our results involving Ru-dye films, Ag-island films without Ru-dye (hereafter called Ag films), and Ag-island films with Ru-dye (Ag/Ru films), we determined the mechanism that controls the enhancement of the Ru-dye absorption.

Material and Methods

To make the Ag/Ru films, first we deposited Ag films of different thickness on either Corning 6059 glass or quartz glass by a vacuum evaporation technique of resistive-heating. We then dispersed various concentrations of Ru-dye solutions (in ethanol) onto the films at either 5.0×10^{-4}, 3.0×10^{-4}, 1.0×10^{-4}, 6.0×10^{-5}, 5.0×10^{-5}, or 3.0×10^{-5} mol/L. We made 18 samples of composite films of various thickness and dye concentration. All samples were dried in a vacuum. The actual concentration of the dye of the Ru-dye film and the Ag/Ru film after drying was calculated using the covered area and the amount of dye dropped onto the substrate. Because the dye concentrations of Ru-dye films and Ag/Ru films were not completely homogeneous, the dye concentration was defined as average value.

The diameter and surface area of the Ag islands were determined using a field emission scanning electron microscope (FESEM, Hitachi S-900). Optical absorption spectra of the Ru-dye films, the Ag films, and the Ag/Ru films were measured in the visible light region (300−850 nm) using a Hitachi U-4000 spectrometer. Photoluminescence spectra of the Ru-dye films and Ag/Ru films were measured at the room temperature using

† University of Tokyo.
‡ AIST.
⊗ Abstract published in *Advance ACS Abstracts,* June 1, 1997.

S1089-5647(96)03931-4 CCC: $14.00

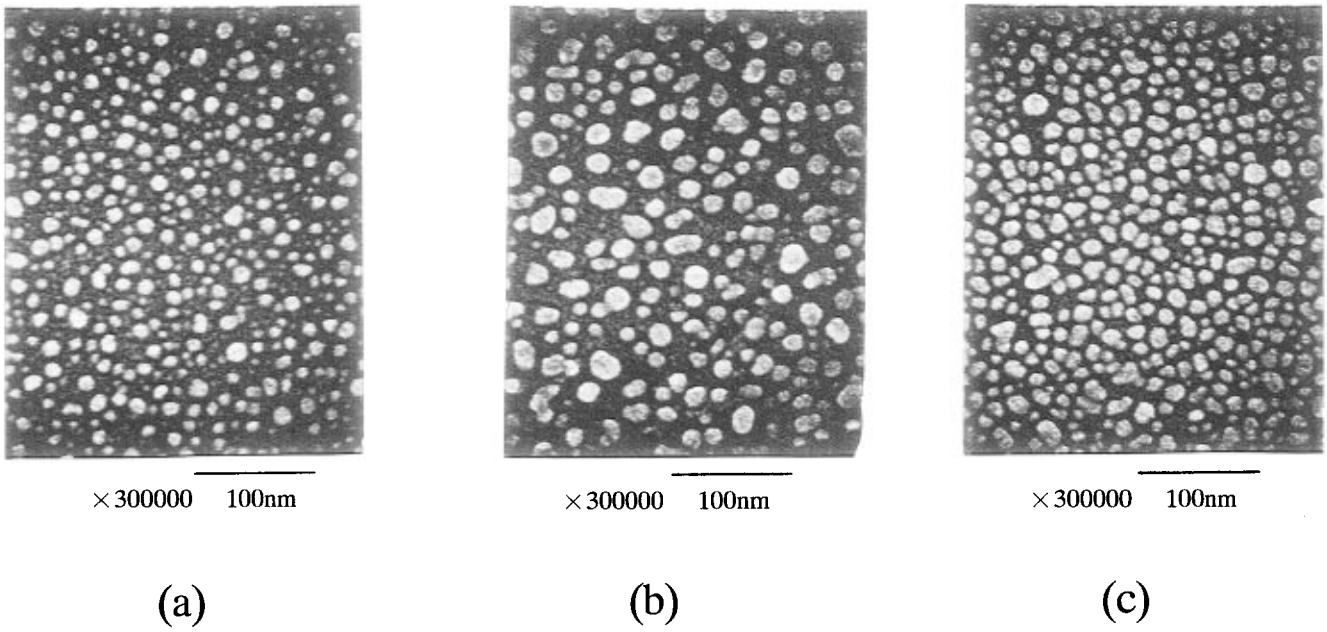

Figure 1. FESEM photographs of Ag-island films: (a) Ag film 1, (b) Ag film 2, and (c) Ag film 6.

TABLE 1: Properties of the Ag-Island Films

	sample no.					
	1	2	3	4	5	6
peak position of Ag surface plasmon adsorption [nm]	471	481	486	499	500	501
average surface area of Ag island per unit area of substrate [cm^2/cm^2]	0.4	0.47	0.40	0.47	0.38	0.63
average diamter of Ag island [nm]	8.5	13.7	5.6	6.2	5.3	9.7

a Jobin-Yvon HR 640 monochromator and GaAs photomultiplier (Hamamatsu Photonics R943−02). An argon laser (514.5 nm) served as the light source. The optical measurements were carried out at the centers of samples. The center parts of samples showed always homogeneous appearances and uniform colors.

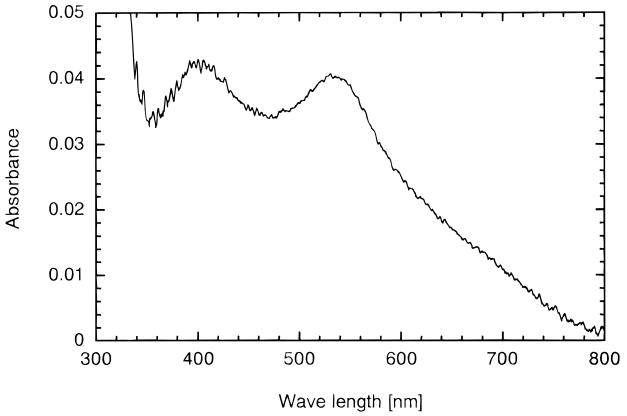

Figure 2. Absorption spectra of *cis*-$Ru(dcb)_2(NCS)_2$ dye for a dye concentration of 8×10^{-9} mol/cm^2.

Results and Discussion

FESEM Photographs of Ag Island Films and the Absorption Spectra of the Ag Films and the Ru-dye Films. FESEM photographs of the Ag films (Figure 1) were used to measure the average diameter of the Ag islands. The average surface area of the Ag islands per unit surface area of substrate was calculated by assuming the island was a hemisphere. The surface plasmon absorption of Ag was evident in the absorption spectra of the Ag films (data not shown). Table 1 lists the average diameter of the Ag islands, the surface plasmon absorption peak position, and the average surface area of the Ag islands. The Ru-dye film has two maximum absorption bands at 400 and 535 nm (Figure 2). Ru-dye exhibits two $\pi \rightarrow \pi^*$ intraligand transitions in the UV and two $t_2 \rightarrow \pi^*$ metal−ligand charge-transfer (MLCT) transitions in the absorption maximum at 396 and 534 nm.[3,23] The absorption band of the maximum at 400 and 535 nm in our experiments correspond to two $t_2 \rightarrow \pi^*$ MLCT transitions. In a Grätzel solar cell, the MLCT transition of the absorption maximum at 396 and 534 nm generates electrons and holes.[1−5] The small absorbance of the molecular Ru-dye at a concentration of 3×10^{-9} mol/cm^2 made the dye on the glass almost transparent to visible light (Figure 3b).

Absorption Enhancement of Ag/Ru Films. The absorption spectra of the Ag/Ru films (Figure 4) show two major absorption bands of the maximum, one around 470−500 nm (hereafter called band A) and one around 520−580 nm (band B). Band A has a peak position and absorbance similar to those for the Ag film used for the Ag/Ru film. Band B is similar to the absorption band of the Ru-dye for the MLCT transition. These results suggest that band A is the surface plasmon absorption of Ag and band B is the significantly enhanced absorption band of the Ru-dye for the MLCT transition, whose absorption maximum is at 400 and 535 nm. The absorption coefficient of band B was 149 times higher than that of Ru-dye. As the Ru-dye concentration was increased, the absorbance at band B increased, and its peak position shifted to longer wavelengths (Figure 4). There was a drastic difference in color among the three films (Figure 3): the Ru-dye film with a concentration of 2×10^{-9} mol/cm^2 was light purple, almost transparent (Figure 3b); the Ag film was brown (Figure 3a); and the Ag/Ru film (Ru-dye concentration of 2×10^{-9} mol/cm^2), which is the Ru-dye film (same as Figure 3b) dispersed on the Ag film (same as Figure 3a) was deep purple (Figure 3c). It means the absorption coefficient of the Ru-dye was greatly enhanced.

Dependence of Absorption Enhancement and Photoluminescence Enhancement on the Ru-dye Concentration. If band B is the Ru-dye MLCT transition of the maximum at 400 and 535 nm that generates electrons and holes, then we can expect improvement in the electric energy conversion efficiency

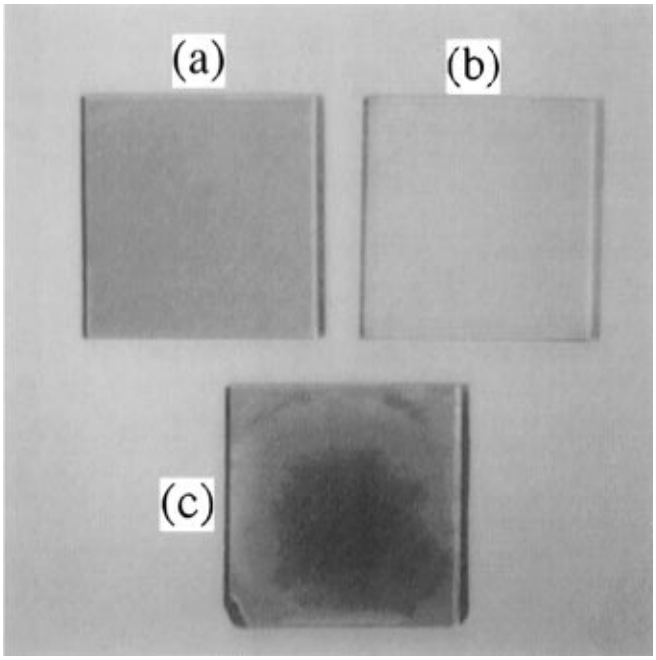

Figure 3. Photographs of (a) Ag film 2, (b) Ru-dye film with a dye concentration of 2×10^{-9} mol/cm^2, and (c) Ag/Ru film with a dye concentration of 2×10^{-9} mol/cm^2 dispersed on Ag film 2.

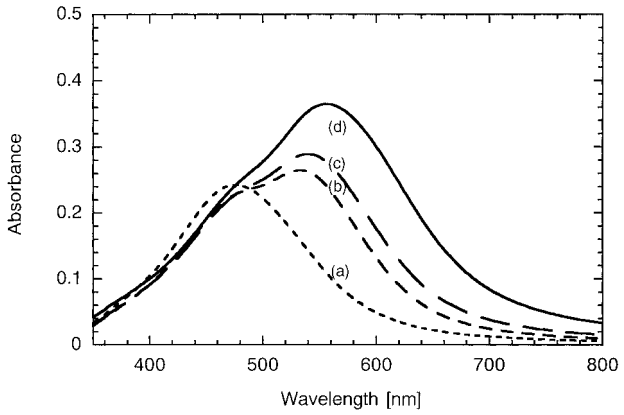

Figure 4. Absorption spectra of Ag/Ru films with a dye concentration of (a) 9×10^{-11} mol/cm^2, (b) 3×10^{-10} mol/cm^2, (c) 5×10^{-10} mol/cm^2, and (d) 2×10^{-9} mol/cm^2.

of dye-sensitized solar cells. Because bands A and B overlapped, we separated the absorption spectra of Ag/Ru films into two Lorentz absorption peaks to clarify the peak positions of each band (Figure 5). The correlation coefficient between the original spectra and the sum of two Lorentz absorption peaks in Figure 5 was 0.9992.

Figure 6 shows the absorbance of band B as a function of Ru-dye concentration. Figure 7 shows the absorption enhancement ratio, which is the ratio of the absorbance for the Ag/Ru film to that for the Ru-dye film. Although the value of absorbance increased with increasing Ru-dye concentration, finally leveling off when the dye concentration reached about 2×10^{-9} mol/cm^2, the absorption enhancement ratio decreased with increasing Ru-dye concentration.

The difference in absorption peak position between the Ag/Ru film (band B) and the Ru-dye film at 535 nm (MLCT transition) increased with increasing Ru-dye concentration, finally leveling off when the concentration reached about 2×10^{-9} mol/cm^2 (Figure 8).

The ratio of the absorbance for the Ag/Ru film (band A) to the absorbance for the Ag film (surface plasmon) decreased with

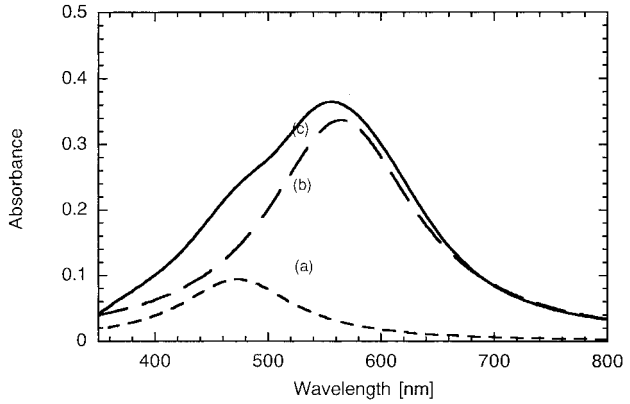

Figure 5. Peak separation of the spectra for an Ag/Ru film (Figure 4d) into two Lorentz absorption peaks: (a) separated peak of absorption band A; (b) separated peak of absorption band B; (c) original peak of the Ag/Ru film.

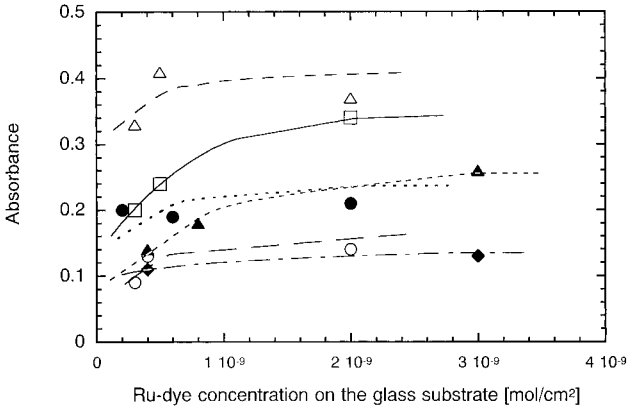

Figure 6. Absorbance of band B versus Ru-dye concentration for (○) Ag film 1, (□) Ag film 2, (◆) Ag film 3, (▲) Ag film 4, (●) Ag film 5, and (△) Ag film 6.

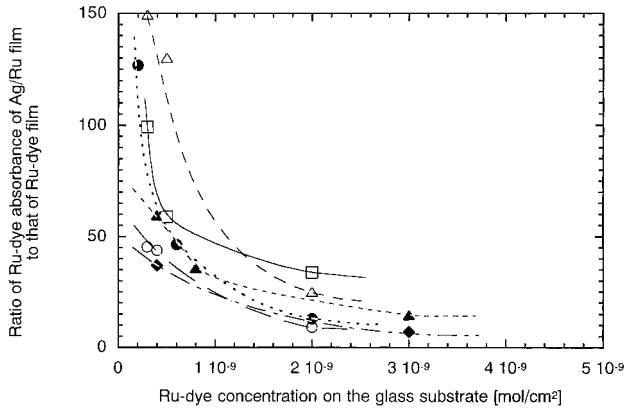

Figure 7. Absorption enhancement ratio versus Ru-dye concentration for (○) Ag film 1, (□) Ag film 2, (◆) Ag film 3, (▲) Ag film 4, (●) Ag film 5, and (△) Ag film 6.

increasing Ru-dye concentration, finally leveling out when the concentration reached about 2×10^{-9} mol/cm^2 (data not shown).

Absorption peak position of Ag-surface plasmon was shifted after the dispersion of the Ru-dye (the difference in Ag plasmon peak between Ag film and Ag/Ru film) and only weakly depended on the Ru-dye concentration (data not shown).

These experimental results can be explained as follows. Band A corresponds to Ag surface plasmon absorption, and band B to the significantly enhanced Ru-dye absorption band for MLCT transition of the maximum at 400 and 535 nm. The absorbance and the absorption peak shift of the band B increased and the absorption enhancement ratio decreased with increasing Ru-

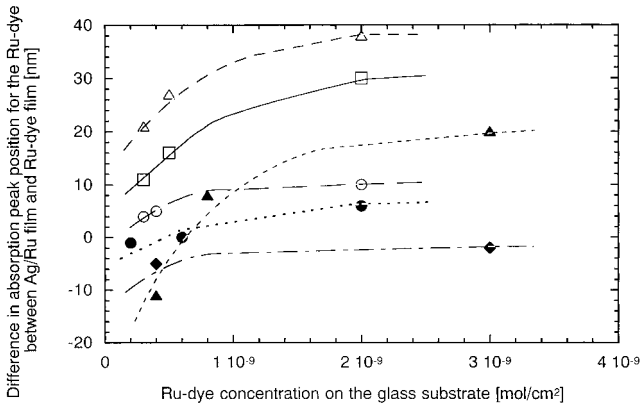

Figure 8. Difference in peak position between absorption band B of Ag/Ru films and the absorption of the Ru-dye film at 535 nm versus Ru-dye concentration. (○) Ag film 1, (□) Ag film 2, (◆) Ag film 3, (▲) Ag film 4, (●) Ag film 5, and (△) Ag film 6.

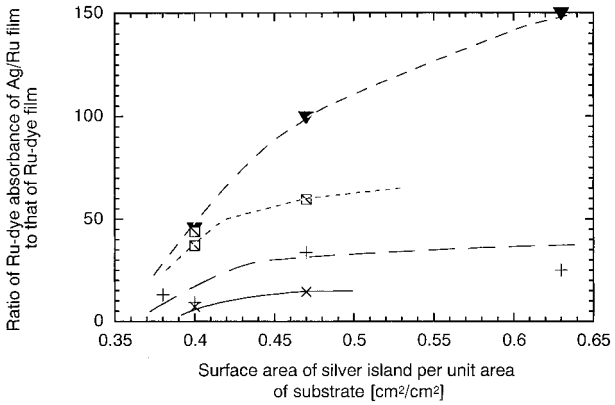

Figure 9. Absorption enhancement ratio versus the average surface area of an Ag island for a Ru-dye concentration (×) of 3×10^{-9} mol/cm^2, (+) 2×10^{-9} mol/cm^2, (□) 4×10^{-10} mol/cm^2, and (▼) 3×10^{-10} mol/cm^2.

dye concentration, up to about 2×10^{-9} mol/cm^2 (Figsures 6−8). These changes relate to the increase in the coverage of the Ru-dye directly adsorbed on the Ag-island surface. The shift of band B was controlled by the amount of the Ru-dye directly adsorbed on Ag, because of the much stronger interaction between Ag and the directly adsorbed Ru-dye than Ag and the indirectly adsorbed dye. The absorbance of band B was also mostly controlled by the amount of Ru-dye directly adsorbed on the surface of the Ag islands, because the absorption coefficient of the noncontacted Ru-dye with Ag should be much smaller than that of the directly adsorbed Ru-dye. The absorption enhancement ratio was governed by the ratio of the amount of Ru-dye directly adsorbed on Ag to that of Ru-dye indirectly adsorbed. The enhancement ratio of band B increased with increasing Ag-island surface area per unit area of substrate and finally became saturated (Figure 9). Furthermore, this saturated surface area of Ag increased with decreasing Ru-dye concentration. This experimental result supports conclusion that the amount of Ru-dye directly adsorbed on Ag controls the enhancement.

A local field enhancement mechanism for the optical responses of molecules in contact with Ag islands is widely accepted.[24−26,16−18] When exposed to light, the surface of each Ag island produces a strong local magnetic field because of a large absorption coefficient for the Ag surface plasmon and of the dipole oscillation that the plasmon produces. The effective absorption strength of the Ru-dye absorbed on an island can be enhanced by the strong local field from the Ag surface. The absorption strength is proportional to the square of the field

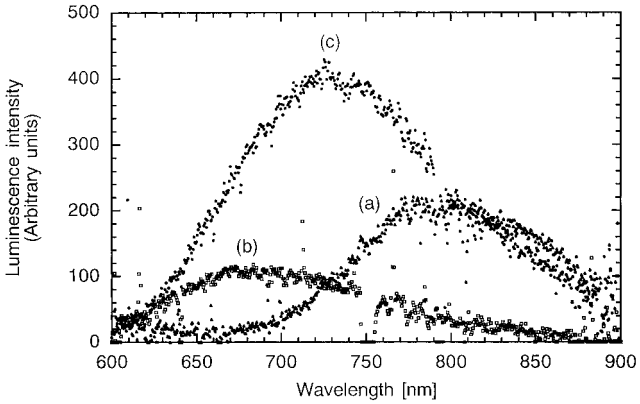

Figure 10. Photoluminescence spectra of (a) Ru-dye film with a dye concentration of 2×10^{-9} mol/cm^2, (b) Ag/ Ru film with a dye concentration of 5×10^{-10} mol/cm^2 dispersed on Ag film 3, and (c) Ag/ Ru film with a dye concentration of 3×10^{-9} mol/cm^2 dispersed on Ag film 3.

intensity. Therefore, in our experiments, the calculated ratio of the local field enhancement for the absorbed Ru-dye ranged from 3 to 12 because the absorption enhancement ratio of the Ru-dye ranged from 7 to 149. The enhanced absorption band of Ru-dye seems to be only one in Ag/Ru film, nevertheless Ru-dye has two absorption peaks (400 and 535 nm) in wavelengths larger than 350 nm. The enhanced absorption band might be the MLCT transition at 535 nm considering the peak position of the enhanced absorption band. However, our results could not indicate exactly which absorption peak was enhanced. If the absorption band at 400 nm are not enhanced, the nonenhanced absorption band should not be detected in spectra of Ag/Ru film because the absorption enhancement ratio was about 100. The mechanism that only the absorption band of 535 or 400 nm was greatly enhanced has not been clarified yet.

For a Ru-dye concentration of 2×10^{-9} mol/cm^2, the coverage of Ru-dye directly adsorbed on Ag islands was maximum, thereby saturating the absorbance increase, the enhancement ratio, and the peak shift of band B. The maximum of the coverage depended on the type of Ag film.

The peak position of the surface plasmon absorption is affected by the adsorption of molecules. In our experiments, the absorption peak position of Ag-surface plasmon was shifted after the dispersion of the Ru-dye (the difference in the Ag plasmon peak between the Ag film and Ag/Ru film) and only weakly depended on the amount of adsorbed Ru-dye.

Figure 10 shows the photoluminescence spectra of the Ru-dye film and the Ag/Ru film. The photoluminescence originated from the MLCT transition of the Ru-dye, and the photoluminescence intensity was enhanced by the Ag islands. The maximum enhancement ratio of the photoluminescence intensity (i.e., the enhancement ratio for the Ag/Ru film to that for the Ru-dye film) achieved in our experiments was 10. Figure 11 shows the difference in the photoluminescence peak position between the Ag/Ru film and the Ru-dye film. The blue-shift in the photoluminescence maximum of the Ag/Ru film, compared with the photoluminescence maximum for the Ru-dye film, decreased with increasing Ru-dye concentration and finally leveled off when the concentration reached about 2×10^{-9} mol/cm^2. The same concentration dependence occurred in the absorbance, the absorption enhancement ratio, and the absorption peak shift. The saturation of the blue-shift was caused by the coverage of Ru-dye directly adsorbed on the Ag islands being maximum. The shift also indicates that band B and the photoluminescence originated from the Ru-dye MLCT transition of the absorption maximum at 400 and 535 nm.

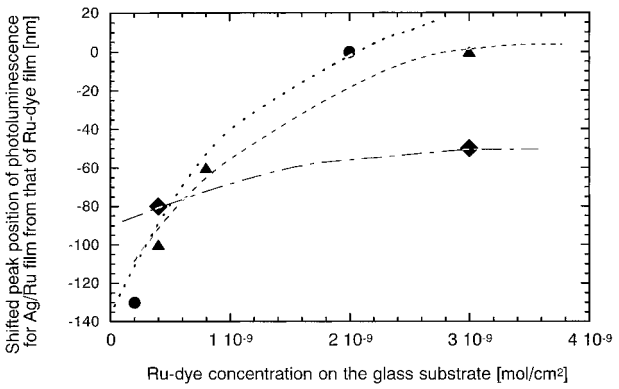

Figure 11. Shift in peak position of photoluminescence for Ag/Ru films at room temperature from that for the Ru-dye film as a function of Ru-dye concentration: (◆) Ag film 3, (▲) Ag film 4, and (●) Ag film 5.

Conclusions

Composite films of Ag islands and *cis*-$(NCS)_2$ bis(2,2′-bipyridyl-4,4′-dicarboxylate)ruthenium(II) dye were fabricated to increase the absorption coefficient of the dye. The Ag islands significantly enhance the absorption coefficient of Ru-dye for the MLCT transition of the absorption maximum at 400 and 535 nm, which generates electrons and holes. This absorption enhancement was controlled by the amount of Ru-dye directly adsorbed on the Ag island. We saw a maximum enhancement of 149 at a dye concentration of 3×10^{-10} mol/cm^2 and a surface area of silver island of 0.63 cm^2/cm^2 of substrate. Such enhancement is expected to improve the energy conversion efficiency of dye-sensitized solar cells, such as the Grätzel cell. This enhancement technique involving Ag islands should be applied to other dyes for possible use in dye-sensitized solar cells.

References and Notes

(1) O'Regan, B.; Grätzel, M. *Nature* **1991**, *353*, 737.
(2) McEvoy, A. J. *Endeavour* **1993**, *17*, 17.
(3) Nazeeruddin, M. K.; Kay, A.; Rodicio, I.; Humphry-Baker, R.; Müller, E.; Liska, P.; Vlachopoulos, N.; Grätzel, M. *J. Am. Chem. Soc.* **1993**, *115*, 6382.
(4) Kay, A.; Grätzel, M. *J. Phys. Chem.* **1993**, *97*, 6272.
(5) Grätzel, M. *Platinum Met. Rev.* **1994**, *38* (4), 151.
(6) Cotton, T. M.; Uphaus, R. A.; Möbius, D. *J. Phys. Chem.* **1986**, *90*, 6071.
(7) Xi, K.; Sharma, S. K.; Muenow, D. W. *J. Raman Spectrosc.* **1992**, *23*, 621.
(8) Kneipp, K.; Hinzmann, G.; Fassler, D. *Chem. Phys. Lett.* **1983**, *99*, 503.
(9) Zhu, Z.; Mao, C.; Yang, R.; Dai, L.; Nie, C. *J. Raman Spectrosc.* **1993**, *24*, 221.
(10) Lippitsch, M. E. *Chem. Phys. Lett.* **1980**, *74*, 125.
(11) Pettinger, B.; Krischer, K.; Ertl, G. *Chem. Phys. Lett.* **1988**, *151*, 151.
(12) Bachackashvilli, A.; Efrima, S.; Katz, B.; Priel, Z. *Chem. Phys. Lett.* **1983**, *94*, 571.
(13) Bachackashvilli, A.; Katz, B.; Priel, Z.; Efrima, S. *J. Phys. Chem.* **1984**, *88*, 6185.
(14) Aroca, R.; Loutfy, R. O. J. *Raman Spectrosc.* **1982**, *12*, 262.
(15) Lee, P. C.; Melsel, D. *J. Phys. Chem.* **1982**, *86*, 3391.
(16) Eagen, C. F. *Appl. Opt.* **1981**, *20*, 3035.
(17) Wang, D.-S.; Kerker, M. *Phys. Rev. B* **1982**, *25*, 2433.
(18) Kerker, M.; Blatchford, C. G. *Phys. Rev. B* **1982**, *26*, 4052.
(19) Glass, A. M.; Liao, P. F.; Bergman, J. G.; Olson, D. H. *Opt. Lett.* **1980**, *5*, 368.
(20) Hartstein, A.; Kirtley, J. R.; Tsang, J. C. *Phys. Rev. Lett.* **1980**, *45*, 201.
(21) Campbell, J. R.; Creighton, J. A. *J. Electroanal Chem.* **1983**, *143*, 353.
(22) Sllman, O.; Lepp, A.; Kerker, M. *J. Phys. Chem.* **1983**, *87*, 5319.
(23) Bryant, G. M.; Fergusson, J. E.; Powell, H. K. J. *Aust. J. Chem.* **1971**, *24*, 257.
(24) Wang, D.-S.; Kerker, M. *Phys. Rev. B* **1981**, *24*, 1777.
(25) Gersten, J.; Nitzan, A. *J. Chem. Phys.* **1980**, *73*, 3023.
(26) Kerker, M.; Wang, D.-S.; Chew, H. *Appl. Opt.* **1980**, *19*, 4159.